

# NOMADS: Non-Markovian Optimization-based Modeling for Approximate Dynamics with Spatially-homogeneous Memory

Ryoji Anzaki and Kazuhiro Sato

**Abstract**—We propose a system identification method, *Non-Markovian Optimization-based Modeling for Approximate Dynamics with Spatially-homogeneous memory (NOMADS)*, for identifying linear dynamical systems from a set of multi-dimensional time-series data obtained through multiple partially excited experiments. NOMADS formulates model identification as a convex optimization problem, in which the state-space coefficient matrices and a memory kernel are estimated jointly under physically motivated constraints using projected gradient descent. The proposed framework models memory effects through a spatially homogeneous kernel, enabling scalable identification of non-Markovian dynamics while keeping the number of free parameters moderate. This structure allows NOMADS to integrate information from multiple multi-dimensional time-series data even when no single experiment provides full excitation. In the Markovian setting, physical constraints can be incorporated to enforce conservation laws. Numerical experiments on synthetic data demonstrate that NOMADS achieves substantially improved generalization accuracy compared to existing DMD-based methods even for noisy train data, and reproduces energy conservation in the Markovian case.

**Index Terms**—Dynamical systems, linear time-invariant system, Non-Markovian dynamics, System identification, Time-series analysis

## I. INTRODUCTION

SYSTEM identification from experimental time-series data is a fundamental problem in science and engineering and underpins prediction and controller design [6]. In high-dimensional systems, however, it is often infeasible to design experiments that sufficiently excite all degrees of freedom. As a result, each experiment typically probes only a subset of the state-input space, yielding *partially excited* time-series data and complicating identification and generalization to unseen conditions.

Dynamic Mode Decomposition (DMD) [13, 15, 12] and its extension DMD with control (DMDc) [9] provide computationally efficient approaches for identifying linear dynamical systems from data. Their effectiveness, however, relies critically on the alignment of excitation between training and

test data; when the excited degrees of freedom in the test data deviate from those explored by the train data, the test prediction error can become unbounded.

When applied to partially excited experiments, DMD-based methods suffer from three fundamental limitations:

- (a) **Limited generalization.** Models identified from insufficient excitation often exhibit rapidly growing prediction errors on unseen test data.
- (b) **Lack of physical consistency.** Prediction may violate known physical properties, such as conservation laws.
- (c) **Neglect of non-Markovian dynamics.** Standard DMD-based formulations rely on Markovian assumptions and cannot adequately represent systems with memory effects or hysteresis.

Limitations (a) and (b) arise from partial excitation, and these limitations may persist even when multiple experiments are available, whereas (c) reflects an intrinsic modeling restriction that becomes critical for systems interacting with an external reservoir or environment [14], such as a thermostat coupled to a heat bath with finite heat capacity.

In this paper, we propose *Non-Markovian Optimization-based Modeling for Approximate Dynamics with Spatially-homogeneous memory (NOMADS)*, a unified identification framework that addresses these challenges. NOMADS integrates information from multiple partially excited trajectories, incorporates memory effects via a low-dimensional memory kernel representation, and enforces physically motivated constraints within a convex optimization formulation. This enables consistent identification of global dynamics even when no single experiment provides full excitation.

The main contributions are as follows:

- 1) We formulate identification of linear dynamical systems with spatially homogeneous memory as a convex optimization problem suited to a set of partially excited multi-trajectory data.
- 2) We develop a projected gradient-based algorithm (NOMADS) and analyze its convexity and convergence properties.
- 3) Numerical experiments demonstrate improved generalization performance and physical consistency compared with existing DMD-based methods for both Markovian and non-Markovian systems, under noiseless and noisy training conditions.

Ryoji Anzaki was with Digital Design Center, Tokyo Electron Ltd., Tokyo, Japan (e-mail: ryo.anzaki+paper@gmail.com).

Kazuhiro Sato is with Graduate School of Information Science and Technology, The University of Tokyo, Tokyo, Japan (e-mail: kazuhiro@mist.i.u-tokyo.ac.jp).

The remainder of the paper is organized as follows. Section II introduces preliminaries, Section III presents the proposed framework, Section IV discusses the optimization algorithm, Section V reports numerical results, and Section VI concludes the paper.

## II. PRELIMINARIES

### A. Metric space of tuples of matrices

Let us denote the set of real numbers, the set of nonnegative real numbers, set of integers and the set of nonnegative integers by  $\mathbf{R}$ ,  $\mathbf{R}_{\geq 0}$ ,  $\mathbf{Z}$ , and  $\mathbf{Z}_{\geq 0}$ , respectively.

For  $\ell, m \in \mathbf{Z}_{\geq 0}$ , define an ordered set of integers  $[\ell : m] := \{\ell, \ell + 1, \ell + 2, \dots, m - 1\} \subset \mathbf{Z}_{\geq 0}$ . We use shorthand notation  $[m] := [0 : m]$ . Note that  $[\ell : m] = \emptyset$  for  $\ell \geq m$ .

For a matrix  $x \in \mathbf{R}^{n \times m}$ , integers  $0 \leq p < q < n$  and  $0 \leq s < t < m$ ,  $x_{p,q,s:t} \in \mathbf{R}^{(q-p) \times (t-s)}$  is a submatrix. We define the similar notation for vectors.

Let us denote a vector by  $\mathbf{v} = (v_i)_{i \in [n]} \in \mathbf{R}^n$  where  $v_i$  is the  $i$ th component. We also denote the same vector but first  $q$  entries are zero by  $(v_i)_{i \in [n]}^q$ . Let us denote  $m \times s$  matrix filled with 0,  $1 \in \mathbf{R}$  by  $0_{m \times s}$  and  $1_{m \times s}$ , and  $m$  dimensional identity matrix by  $\mathbb{1}_m$ . For a matrix  $A$ , we denote the transposed matrix by  $A^\top$  and the Moore-Penrose pseudoinverse by  $A^+$ . We also denote  $A = (A_{ij})$  where  $i, j$  are row and column indices, respectively. If  $A$  is a square matrix, we denote the trace (sum of diagonal elements) of the matrix by  $\text{tr}(A)$ .

For matrices  $A, A'$  of the same shape, let us introduce the inner product by

$$\langle A, A' \rangle := \text{tr}(A^\top A'). \quad (1)$$

This inner product induces the Frobenius norm  $\|A\| = \sqrt{\text{tr}(A^\top A)}$ . For a pair of tuple of matrices of the same shapes  $\mathbf{A} := (A_0, \dots, A_{n-1})$  and  $\mathbf{A}' := (A'_0, \dots, A'_{n-1})$  where  $A_i, A'_i \in \mathbf{R}^{n_i \times m_i}$  for  $i \in [n]$ , we define

$$\langle \mathbf{A}, \mathbf{A}' \rangle := \sum_{i \in [n]} \text{tr}(A_i^\top A'_i). \quad (2)$$

The inner product induces the norm of a tuple of matrices as follows:

$$\|\mathbf{A}\| := \sqrt{\langle \mathbf{A}, \mathbf{A} \rangle}. \quad (3)$$

### B. Causal Matrices

In this subsection, we prepare the basic concepts to define linear dynamical systems with homogeneous memory in the next section. The definitions below are useful when dealing with dynamical systems whose state vectors at the first  $q + 1$  ( $q \in \mathbf{Z}_{\geq 0}$ ) time points are given.

For a function  $h : [m] \rightarrow \mathbf{R}$  of time  $t$ , define *time-ordered vector* as  $\mathsf{T}_h([m]) = (h(0), h(1), \dots, h(m-1))$ .

*Definition 1 (Causal matrix):* A matrix  $C \in \mathbf{R}^{m \times m}$  is called causal matrix if  $C$  satisfies the following properties for an integer  $q \geq 0$ :

- $C_{:,q} = 0_{m \times q}$
- $C_{q,q}$  is an invertible upper-triangular matrix

A causal matrix is a discrete representation of a causal linear operator defined in [1]. It is called *causal*, because a vector-matrix multiplication with a causal matrix does not violate

the causality for a time-ordered vector, i.e., the multiplication results in the weighted sum of *past* elements of the original vector  $\mathsf{T}_h([m])$  for each element: for  $t > q$ ,

$$(\mathsf{T}_h([m])^\top C)_t = \sum_{t' \in [q:t]} C_{tt'} h(t'). \quad (4)$$

*Definition 2 (Time-invariant causal matrix):* A matrix  $C \in \mathbf{R}^{m \times m}$  is called *time-invariant causal matrix* if  $C$  satisfies the following property: in addition to the properties shown in Definition 1, there is a  $m$ -dimensional Toeplitz matrix  $T \in \mathbf{R}^{m \times m}$  such that  $C_{:,q} = T_{:,q}$ .

A time-invariant causal matrix is called time-invariant because  $C_{t,s} = C_{t+\delta t, s+\delta t}$ .

*Definition 3:* Assume that  $C \in \mathbf{R}^{m \times m}$  is a time-invariant causal matrix with nullity  $q$  (i.e., in this case, the first  $q$  columns are zero). We say that  $C$  is normalized if the diagonal elements of  $C_{q,q}$  are unity.

Let us denote the set of  $m$ -dimensional normalized time-invariant causal matrices with nullity  $q$  by  $\mathbb{T}_m^q$ . Also, we use a shorthand notation

$$\mathbb{1}_m^q := \begin{pmatrix} 0_{q \times q} & 0_{q \times (m-q)} \\ 0_{(m-q) \times q} & \mathbb{1}_{m-q} \end{pmatrix}. \quad (5)$$

*Lemma 4:* The left pseudoinverse<sup>1</sup> of  $C \in \mathbb{T}_m^q$  is given as follows:

$$C^+ = \begin{pmatrix} 0_{q \times q} & 0_{q \times (m-q)} \\ 0_{(m-q) \times q} & (C_{q,q})^{-1} \end{pmatrix}. \quad (6)$$

Note that, for a matrix  $C \in \mathbb{T}_m^q$ , the left pseudoinverse  $C^+$  defined above is not the right pseudoinverse of  $C$  in general:

$$CC^+ = \begin{pmatrix} 0_{q \times q} & C_{q,q}(C_{q,q})^{-1} \\ 0_{(m-q) \times q} & \mathbb{1}_{m-q} \end{pmatrix}. \quad (7)$$

We denote the subset of  $\mathbb{T}_m^q$  whose elements has bandwidth  $Q$  by  $\mathbb{T}_m^q(Q)$ . Namely, for a matrix  $(c_{i,j}) \in \mathbb{T}_m^q(Q)$ ,  $c_{i-k,i}$  is nonzero only if  $k \in [\max(Q, i)]$  for  $i \in [m]$ .

The following theorem is useful to show the convergence of optimization problem for  $C \in \mathbb{T}_m^q(Q)$ . The proof is straightforward and thus omitted.

*Theorem 5:* Assume  $Q \geq 0$ ,  $Q \geq q \geq 0$ , and  $m \geq Q$  are integers.  $\mathbb{T}_m^q(Q)$  is a convex and closed subset of  $\mathbf{R}^{m \times m}$ .

## III. PROBLEM SETTINGS

In this section, we formulate the system identification in NOMADS. We first introduce a class of non-Markovian dynamical systems, and then postulate the system identification as an optimization problem using multiple multi-dimensional time-series data.

### A. Linear Dynamical Systems with Homogeneous Memory

In this section, we consider discrete-time dynamical systems with states  $\mathbf{x}_t \in \mathbf{R}^n$  and inputs  $\mathbf{u}_t \in \mathbf{R}^k$  for  $t \in \mathbf{Z}_{\geq 0}$ . We introduce a class of linear non-Markovian models with *spatially-homogeneous memory* (hereafter referred to as homogeneous

<sup>1</sup>For a matrix  $A \in \mathbf{R}^{n \times n}$ , a left (right) pseudoinverse  $L \in \mathbf{R}^{n \times n}$  ( $R \in \mathbf{R}^{n \times n}$ ) is a matrix that satisfies  $LA = \mathbb{1}_n^q$  ( $AR = \mathbb{1}_n^q$ ) where  $q$  is the nullity of  $A$ .

memory), which forms the modeling basis of the proposed method.

*Definition 6: (Linear dynamical systems with homogeneous memory):* Assume that  $q + 1$  initial states  $(\mathbf{x}_t)_{t \in [q+1]}$  and inputs  $(\mathbf{u}_t)_{t \in [m]}$  with  $m \geq q$  are given. For  $t \in [q + 1, m + 1]$ , the state evolution satisfies

$$YD = AX + BU, \quad (8)$$

where  $(A, B, D) \in \mathbf{R}^{n \times n} \times \mathbf{R}^{n \times k} \times \mathbb{T}_m^q(Q)$ . Here,

$$X = (\mathbf{x}_t)_{t \in [m]}^q \in \mathbf{R}^{n \times m}, \quad Y = (\mathbf{x}_{t+1})_{t \in [m]}^q \in \mathbf{R}^{n \times m}, \quad (9)$$

$$U = (\mathbf{u}_t)_{t \in [m]}^q \in \mathbf{R}^{k \times m}, \quad (10)$$

and  $D$  has embedding dimension  $1 \leq Q \leq m$ . We call (8) a *linear dynamical system with homogeneous memory*, and refer to  $D$  as the *memory kernel matrix*.

This class of dynamical system is said to have *homogeneous memory* because the memory kernel is spatially homogeneous (independent of the spatial degree of freedom).

*Remark 7 (Constraint):* In some cases, we have *a priori* knowledge on the coefficient matrices  $A, B, D$  in the linear dynamical systems with homogeneous memory (8), and we can reflect the knowledge to the set of parameters. For example, if we know that all the elements in  $A$  are nonnegative, we can impose a *constraint*  $A \in (\mathbf{R}_{\geq 0})^{n \times n}$ .

In general, an *a priori* knowledge leads to a constraint of the form  $(A, B, D) \in \mathbb{E}$  where  $\mathbb{E}$  is a subset of  $\mathbf{R}^{n \times n} \times \mathbf{R}^{n \times k} \times \mathbb{T}_m^q(Q)$ . If the subset  $\mathbb{E}$  is a closed convex subset, the analysis of the constraint becomes easy. We list some of the closed convex constraints below:

- Element-wise equality: e.g.,  $A_{ii} = 0$  for  $i \in [n]$
- Element-wise inequality: e.g.,  $A_{ii} \geq 0$  for  $i \in [n]$
- Symmetry: e.g.,  $A = A^\top$

### B. Linear Systems with Homogeneous Memory and ARX Models

A linear dynamical systems with homogeneous memory (8) is transformed to an autoregressive exogenous (ARX) model. For  $t \in [q + 1 : m]$ ,

$$\mathbf{x}_t = A\mathbf{x}_{t-1} - \sum_{k \in [1:Q]} d_{t-k,t} \mathbf{x}_{t-k} + B\mathbf{u}_{t-1}, \quad (11)$$

where  $Q$  is the embedding dimension,  $D = (d_{ij})$  and  $\mathbf{x}_t = 0_{n \times 1}$  for  $t < 0$ .

The model can be further transformed into a Hankelized state-space representation by stacking snapshot vectors to form extended state variables [13]. However, this increases the state dimension from  $n$  to  $Qn$ , leading to coefficient matrices of size  $Qn \times Qn$  and a computational cost that scales as  $\mathcal{O}((Qn)^3)$  when pseudoinverse-based identification is employed.

### C. Identification of Dynamical Systems

In large-scale systems, fully exciting all degrees of freedom through experiments is rarely feasible. As a result, each experiment typically excites only a subset of the state-input space, yielding *partially excited* trajectories.

Under partial excitation, system identification becomes ill-posed. For a single trajectory, the snapshot matrix  $X$  and input matrix  $U$  generally span a low-dimensional subspace, so that the regression matrix  $(X^\top, U^\top)^\top$  is not full row rank. This issue is directly reflected in the DMDC regression

$$\min_{(A \ B) \in \mathbf{R}^{n \times (n+k)}} \left\| Y - (A \ B) \begin{pmatrix} X \\ U \end{pmatrix} \right\|, \quad (12)$$

which admits infinitely many solutions whenever  $(X^\top, U^\top)^\top$  is rank-deficient:

$$(A \ B) = Y \begin{pmatrix} X \\ U \end{pmatrix}^+ + M \left( \mathbb{1}_{n+k} - \begin{pmatrix} X \\ U \end{pmatrix} \begin{pmatrix} X \\ U \end{pmatrix}^+ \right), \quad (13)$$

with an arbitrary matrix  $M \in \mathbf{R}^{n \times (n+k)}$ , which is set to zero in DMDC framework. Only when  $(X^\top \ U^\top)^\top$  is full row rank (corresponding to a fully excited experiment in the noiseless case) does the solution become unique.

A common approach is to aggregate multiple experiments by stacking the data,  $X = (X_\mu)_{\mu \in [N]}$ ,  $X' = (X'_\mu)_{\mu \in [N]}$ ,  $U = (U_\mu)_{\mu \in [N]}$ , which can alleviate rank deficiency caused by individual trajectories, and is equivalent to multi-trajectory DMDC [2] without constraints. However, in high-dimensional systems, even this multi-trajectory approach may remain insufficient, and naive stacking alone does not ensure reliable generalization.

The difficulty is more pronounced for non-Markovian systems. Although ARX models [3] and Hankelized representations (Section III-B) can represent memory effects, their parameter dimension grows rapidly with system size or memory length, and incorporating physical constraints is generally nontrivial.

These observations motivate a modeling framework that (i) systematically exploits multiple partially excited trajectories and (ii) directly incorporates physical constraints into the identification problem of non-Markovian dynamical systems, which is the focus of the proposed NOMADS framework.

### D. Statement of Problem in NOMADS

In this subsection, we formulate the system identification problem addressed by NOMADS as a constrained optimization problem. We consider multiple time-series trajectories obtained from possibly different experimental conditions, and seek to identify a single global dynamical model that is consistent with all trajectories while incorporating structural or physical constraints.

Assume we have a set of tuples of time-series data  $\mathcal{D}_N$  defined below:

$$\mathcal{D}_N := \left\{ \mathcal{D}^{(\mu)} \mid \mu \in [N] \right\}, \quad (14)$$

$$\mathcal{D}^{(\mu)} := \left( \left( \mathbf{x}_t^{(\mu)} \right)_{t \in [m_\mu]}, \left( \mathbf{u}_t^{(\mu)} \right)_{t \in [m_\mu]} \right). \quad (15)$$

Each  $\mathcal{D}^{(\mu)}$  is called a *trajectory*, and  $N$  denotes the number of trajectories. The integer  $m_\mu > 2$  represents the length of the  $\mu$ -th trajectory. We fix a positive integer  $m < \min_\mu (m_\mu) - 1$ , which determines the number of snapshots used for identification.

TABLE I  
DMD-BASED METHODS.

Method	$Y$	$U$	$q$	$\text{St}(A)$	$\text{St}(B)$	$\text{St}(D)$
DMD [15]	$X'$	0	0	$\mathbf{R}^{n \times n}$	$\{0\}$	$\{\mathbb{1}_m\}$
DMDc [9]	$X'$	$U$	0	$\mathbf{R}^{n \times n}$	$\mathbf{R}^{n \times k}$	$\{\mathbb{1}_m\}$
DMDm [1]	$X^0$	$U$	$q$	$\mathbf{R}^{n \times n}$	$\mathbf{R}^{n \times k}$	$\mathbb{T}_m^q$

We consider the following optimization problem:

$$\begin{aligned} \text{Minimize } f(A, B, D) &:= \sum_{\mu=0}^{N-1} \|Y_\mu D - (AX_\mu + BU_\mu)\|^2 \\ \text{subject to } (A, B, D) &\in \text{St}(A) \times \text{St}(B) \times \text{St}(D), \end{aligned} \quad (16)$$

where

$$X_\mu = \begin{pmatrix} 0_{n \times q} & \mathbf{x}_q^{(\mu)} & \mathbf{x}_{q+1}^{(\mu)} & \cdots & \mathbf{x}_{m-1}^{(\mu)} \end{pmatrix} \in \mathbf{R}^{n \times m}, \quad (17)$$

$$Y_\mu = \begin{pmatrix} 0_{n \times q} & \mathbf{x}_{q+1}^{(\mu)} & \mathbf{x}_{q+2}^{(\mu)} & \cdots & \mathbf{x}_m^{(\mu)} \end{pmatrix} \in \mathbf{R}^{n \times m}, \quad (18)$$

$$U_\mu = \begin{pmatrix} 0_{n \times q} & \mathbf{u}_q^{(\mu)} & \mathbf{u}_{q+1}^{(\mu)} & \cdots & \mathbf{u}_{m-1}^{(\mu)} \end{pmatrix} \in \mathbf{R}^{k \times m}, \quad (19)$$

are data matrices constructed from each trajectory.

The sets  $\text{St}(A) \subseteq \mathbf{R}^{n \times n}$ ,  $\text{St}(B) \subseteq \mathbf{R}^{n \times k}$ , and  $\text{St}(D) \subseteq \mathbb{T}_m^q$  are closed convex subsets encoding *a priori* knowledge of the system parameters, as discussed in Remark 7. We denote the feasible set by  $\mathbb{E} := \text{St}(A) \times \text{St}(B) \times \text{St}(D)$ .

An optimal solution to (16) is expected to exist in practice, since  $\mathbb{E}$  can be chosen as a bounded set. For reference, we also define the unconstrained parameter space  $\mathbb{E}_0 := \mathbf{R}^{n \times n} \times \mathbf{R}^{n \times k} \times \mathbb{T}_m^q$ .

The identification problem (16) is formulated to handle collections of experiments in which each trajectory may be only partially excited. The identified model admits an ARX-type representation via (11), while keeping the number of free parameters bounded by  $n^2 + nk + m$ , which is smaller than that of standard ARX models or Hankelized state-space representations.

This reduction follows from the assumption of *spatially homogeneous memory*. While this structural assumption enables scalable identification under partial excitation, it may limit approximation accuracy when the true memory kernel exhibits strong spatial heterogeneity.

*Remark 8:* If  $\mathbb{E} = \mathbb{E}_0$ , we refer to (16) as an *unconstrained* optimization problem. If  $\mathbb{E} \subsetneq \mathbb{E}_0$ , it is called a *constrained* optimization problem. The latter corresponds to system identification with structural or physical constraints.

*Remark 9:* Several existing DMD-based methods can be recovered as special cases of (16), as summarized in Table I. We use the shorthand notation  $X' = (\mathbf{x}_{t+1})_{t \in [m]}$ ,  $X^0 = (\mathbf{x}_t)_{t \in [m]}$ .

#### IV. CONVEX OPTIMIZATION SCHEME

This section presents a convex optimization algorithm NO-MADS for solving (16). We show that the loss function is convex and Lipschitz smooth, enabling the use of projected gradient descent (PGD) with a global sublinear convergence rate.

#### A. Properties of the Optimization Problem

In this subsection, we analyze fundamental properties of the optimization problem (16). In particular, we derive explicit expressions for the gradient and Hessian of the loss function, and establish convexity and smoothness, which form the theoretical basis for the PGD algorithm.

*Theorem 10:* The gradient  $\nabla f(A, B, D)$  and the Hessian  $\text{Hess}f(A, B, D)$  of the function  $f$  are given by the followings:

$$\nabla f(A, B, D) = \sum_{\mu=0}^{N-1} (-2E_\mu X_\mu^\top, -2E_\mu U_\mu^\top, 2Y_\mu^\top E_\mu), \quad (20)$$

where  $E_\mu = Y_\mu D - (AX_\mu + BU_\mu)$ , and

$$\begin{aligned} \text{Hess}f(A, B, D)[(\Delta_A, \Delta_B, \Delta_D)] \\ = \sum_{\mu=0}^{N-1} (-2e_\mu X_\mu^\top, -2e_\mu U_\mu^\top, 2Y_\mu^\top e_\mu), \end{aligned} \quad (21)$$

where  $e_\mu = Y_\mu \Delta_D - (\Delta_A X_\mu + \Delta_B U_\mu)$ . Also, the loss function  $f$  is a convex function.

*Proof:* First we prove the expression for the gradient. For  $(\Delta_A, \Delta_B, \Delta_D) \in \mathbf{R}^{n \times n} \times \mathbf{R}^{n \times k} \times \mathbf{R}^{m \times m}$ , using the definitions (1) and (3),

$$\begin{aligned} f(A + \Delta_A, B + \Delta_B, D + \Delta_D) - f(A, B, D) \\ = 2 \sum_{\mu=0}^{N-1} (-\text{tr}(E_\mu^\top \Delta_A X_\mu) - \text{tr}(E_\mu^\top \Delta_B U_\mu) + \text{tr}(E_\mu^\top Y_\mu \Delta_D)) \\ + \mathcal{O}(\Delta_A^2 + \Delta_B^2 + \Delta_D^2). \end{aligned} \quad (22)$$

Use of the identities  $\text{tr}(E_\mu^\top \Delta_A X_\mu) = \text{tr}(X_\mu E_\mu^\top \Delta_A)$  and  $\text{tr}(E_\mu^\top \Delta_B U_\mu) = \text{tr}(U_\mu E_\mu^\top \Delta_B)$  yields the expression for the gradient (20).

Second, we prove the expression for Hessian. Noting that the Hessian is the gradient of  $\nabla f(A, B, D)$  and

$$\begin{aligned} \nabla f(A + \Delta_A, B + \Delta_B, D + \Delta_D) - \nabla f(A, B, D) \\ = \sum_{\mu=0}^{N-1} (-2e_\mu X_\mu^\top, -2e_\mu U_\mu^\top, 2Y_\mu^\top e_\mu), \end{aligned} \quad (23)$$

we obtain (21). Third, we show the convexity of  $f$ . From (1) and (21),

$$\begin{aligned} \langle \text{Hess}f(A, B, D)[(\Delta_A, \Delta_B, \Delta_D)], (\Delta_A, \Delta_B, \Delta_D) \rangle \\ = 2 \sum_{\mu=0}^{N-1} \|e_\mu\|^2 \geq 0. \end{aligned} \quad (24)$$

Therefore, the loss function  $f$  is a convex function [10]. ■

Note that, the Hessian is a *sum over trajectories* and we can enhance the condition number of the Hessian by adding new trajectories.

In many applications, we are interested in the uniqueness of the coefficient matrices.

*Theorem 11:* The optimization problem (16) has a unique minimizer if  $\text{Hess}f(A, B, D)$  is positive definite.

*Proof:* The function  $f$  is a strongly convex function, because  $\text{Hess}f(A, B, D)$  is positive definite. Thus, the sub-level set of  $f$  is a bounded subset. This implies that the optimization problem (16) has a unique minimizer [5]. ■

---

**Algorithm 1** Algorithm for NOMADS
 

---

**Require:** initial stepsize  $t_0 > 0$ , constant  $\eta > 1$ , initial guess  $\theta^{(0)} \in \mathbb{E}_0$ , convex projection  $\mathcal{P}_{\mathbb{E}}$  onto  $\mathbb{E} \subset \mathbb{E}_0$ , maximum number of steps  $p \geq 1$

- 1: **for**  $\ell = 0$  to  $p - 1$  **do**
- 2:    $\theta' \leftarrow \mathcal{P}_{\mathbb{E}}(\theta^{(\ell)} - t_\ell \nabla f(\theta^{(\ell)}))$
- 3:    $f' \leftarrow f(\theta^{(\ell)}) + \langle (\theta' - \theta^{(\ell)}), \nabla f(\theta^{(\ell)}) \rangle + (2t_\ell)^{-1} \|\theta' - \theta^{(\ell)}\|^2$
- 4:   **while**  $f(\theta') > f'$  **do**
- 5:      $t_\ell \leftarrow t_\ell / \eta$
- 6:      $\theta' \leftarrow \mathcal{P}_{\mathbb{E}}(\theta^{(\ell)} - t_\ell \nabla f(\theta^{(\ell)}))$
- 7:      $f' \leftarrow f(\theta^{(\ell)}) + \langle (\theta' - \theta^{(\ell)}), \nabla f(\theta^{(\ell)}) \rangle + (2t_\ell)^{-1} \|\theta' - \theta^{(\ell)}\|^2$
- 8:   **end while**
- 9:    $\theta^{(\ell+1)} \leftarrow \theta'$
- 10:  $t_{\ell+1} \leftarrow t_\ell$
- 11: **end for**
- 12: **return**  $\theta^{(p)}$

---

In general, the minimizer of (16) is not unique, because the Hessian (21) has nonempty kernel.

*Remark 12:* In general, the Hessian (21) cannot be expressed as a matrix, because it contains linear maps  $\mathbf{R}^{a \times b} \rightarrow \mathbf{R}^{c \times d}$  of the form  $\sigma_{P,Q} : M \mapsto PMQ$  for given matrices  $P \in \mathbf{R}^{c \times a}$ ,  $Q \in \mathbf{R}^{b \times d}$  and for any matrix  $M \in \mathbf{R}^{a \times b}$ . On the other hand, when the set for the memory kernel is a singleton, i.e.,  $\text{St}(D) = \{D\}$ , the Hessian admits a matrix representation. In this case, the Hessian with respect to  $(A, B)$  is given by

$$H(A, B) = \sum_{\mu=0}^{N-1} \begin{pmatrix} X_\mu X_\mu^\top & X_\mu U_\mu^\top \\ U_\mu X_\mu^\top & U_\mu U_\mu^\top \end{pmatrix}, \quad (25)$$

which coincides with the Hessian obtained in [2].

## B. Projected Gradient Descent Method

We can solve the optimization problem (16) using PGD method shown in Algorithm 1. We call Algorithm 1 NOMADS, standing for *Non-Markovian Optimization-based Modeling for Approximate Dynamics with Spatially-homogeneous memory*.

In Algorithm 1, the convex projection  $\mathcal{P}_{\mathbb{E}}$  onto  $\mathbb{E}$  is defined as

$$\mathcal{P}_{\mathbb{E}} : \theta \mapsto \arg \min_{\vartheta \in \mathbb{E}} \|\theta - \vartheta\|. \quad (26)$$

The exact form of the projection operator  $\mathcal{P}_{\mathbb{E}}$  depends on the space  $\mathbb{E}$  [4]. Using (3) and the fact that  $\text{St}(A), \text{St}(B)$ , and  $\text{St}(D)$  are closed convex sets, we can see that for the convex projection (26) there exists a unique tuple of convex projections  $\mathcal{P}_{\text{St}(A)} : \mathbf{R}^{n \times n} \rightarrow \text{St}(A)$ ,  $\mathcal{P}_{\text{St}(B)} : \mathbf{R}^{n \times k} \rightarrow \text{St}(B)$ , and  $\mathcal{P}_{\text{St}(D)} : \mathbf{R}^{m \times m} \rightarrow \text{St}(D)$  that satisfies:

$$\mathcal{P}_{\mathbb{E}}(A, B, D) = (\mathcal{P}_{\text{St}(A)}(A), \mathcal{P}_{\text{St}(B)}(B), \mathcal{P}_{\text{St}(D)}(D)). \quad (27)$$

For a matrix  $D \in \mathbf{R}^{m \times m}$ , the convex projection

$\mathcal{P}_{\mathbb{T}_m^q(Q)}(D) = (E_{ij}) \in \mathbf{R}^{m \times m}$  is expressed as:

$$E_{ij} = \begin{cases} 0 & i > j \\ (m_{ij} - q_{ij})^{-1} \sum_{k=q_{ij}}^{m_{ij}-1} D_{k, k+(j-i)} & i \leq j < i + Q, \\ 0 & j \geq i + Q \end{cases}, \quad (28)$$

where  $m_{ij} = m - (j - i)$  and  $q_{ij} = \max(0, q - (j - i))$ . Note that the projection  $\mathcal{P}_{\mathbb{T}_m^q(Q)}$  can be defined due to Theorem 5.

The function  $f$  is Lipschitz smooth as shown in the following theorem, which is used in the proof of Theorem 14.

*Theorem 13 (Lipschitz smoothness of  $f$ ):* In the optimization problem (16), the function  $f$  is  $L_f$ -smooth on  $\mathbb{E}_0$ , where

$$L_f := 2 \sum_{\mu=1}^N (\|X_\mu\|^2 + \|U_\mu\|^2 + \|Y_\mu\|^2). \quad (29)$$

*Proof:* Since the Hessian operator (21) is a constant operator  $\text{Hess}f$  independent of  $(A, B, D)$ ,

$$\|\nabla f(\theta') - \nabla f(\theta)\| \leq \|\text{Hess}f\| \|\theta - \theta'\|, \quad (30)$$

for any  $\theta = (\Delta_A, \Delta_B, \Delta_D)$ ,  $\theta' \in \mathbb{E}_0$ . Here  $\|\text{Hess}f\|$  denotes the operator norm induced by the Frobenius norm.

For nonzero  $(\Delta_A, \Delta_B, \Delta_D)$ ,

$$\begin{aligned} & \frac{\|\text{Hess}f[(\Delta_A, \Delta_B, \Delta_D)]\|}{\|(\Delta_A, \Delta_B, \Delta_D)\|} \\ &= \sqrt{\frac{4 \sum_{\mu=1}^N \|e_\mu\|^2 (\|X_\mu\|^2 + \|U_\mu\|^2 + \|Y_\mu\|^2)}{\|(\Delta_A, \Delta_B, \Delta_D)\|^2}} \\ &\leq 2 \sum_{\mu=1}^N (\|X_\mu\|^2 + \|U_\mu\|^2 + \|Y_\mu\|^2), \end{aligned} \quad (31)$$

where we used

$$\begin{aligned} \|e_\mu\|^2 &= (\|\Delta_A\|^2 \|X_\mu\|^2 + \|\Delta_B\|^2 \|U_\mu\|^2 + \|\Delta_D\|^2 \|Y_\mu\|^2) \\ &\leq \|(\Delta_A, \Delta_B, \Delta_D)\|^2 (\|X_\mu\|^2 + \|U_\mu\|^2 + \|Y_\mu\|^2) \end{aligned} \quad (32)$$

Therefore  $\|\text{Hess}f\| \leq L_f$ , meaning,

$$\|\nabla f(\theta') - \nabla f(\theta)\| \leq L_f \|\theta - \theta'\|, \quad (33)$$

for any  $\theta, \theta' \in \mathbb{E}_0$ . ■

Now we show the convergence of Algorithm 1.

*Theorem 14 (Convergence of the PGD algorithm):*

Assume that (16) has an optimal solution. If  $p = \infty$ , Algorithm 1 generates a sequence of parameters  $\theta_\ell \in \mathbb{E}$  ( $\ell \in \mathbf{Z}_{\geq 1}$ ) that converges to an optimal solution of problem (16).

*Proof:* From Theorem 13, the function  $f$  is  $L_f$ -smooth for (29). We can also show that  $f(\theta) \geq 0$  for any  $\theta \in \mathbb{E}$ , and that there exists a  $\theta \in \mathbb{E}$  such that  $f(\theta) < \infty$  provided that the data matrices  $X_\mu, Y_\mu, U_\mu$  and the number of trajectories  $N$  are finite. Using Theorem 10.24 in [4], we can show the convergence of Algorithm 1. ■

We can remove the assumption that (16) has an optimal solution, if the set of parameters  $\mathbb{E}$  in the optimization problem (16) is bounded.

*Remark 15:* In case the constrained parameter space  $\mathbb{E}$  is not a convex subset of  $\mathbb{E}$ , Algorithm 1 will generate a sequence of parameters  $\theta_\ell \in \mathbb{E}$  ( $\ell \in \mathbf{Z}_{\geq 1}$ ) that converges to a stationary point of the objective function  $f$ .

*Remark 16:* Although the convergence of NOMADS is assured even if we use a constant stepsize  $1/L_f \geq t > 0$  [4], we expect a better behavior by *adjusting* stepsize as shown in Algorithm 1 because the Lipschitz constant  $L_f$  is often a huge real number depending on the data (14).

*Theorem 17 (Convergence rate of NOMADS):* Assume that problem (16) has an optimal solution. Then Algorithm 1 converges at a sublinear rate  $O(1/\ell)$ .

*Proof:* By Theorem 13, the objective function  $f$  is convex with a Lipschitz continuous gradient, and the feasible set  $\mathbb{E} = \text{St}(A) \times \text{St}(B) \times \text{St}(D)$  is closed and convex. Thus, Algorithm 1 is an instance of projected gradient descent for a smooth convex optimization problem. The stated convergence rate follows from [8]. ■

## V. NUMERICAL EXPERIMENTS

We conduct numerical experiments on synthetic data to evaluate NOMADS, focusing on *generalization performance* under *partially excited* experiments, motivated by multi-zone thermostat dynamics with heat exchange with the environment. Models are trained on multiple synthetic data and evaluated on unseen test data, reflecting the challenges discussed in Section III-C.

### A. Experimental Set-ups

We consider a synthetic benchmark defined on a two-dimensional grid  $[L_x] \times [L_y]$  with periodic boundary conditions in the first direction, corresponding to a cylindrical topology. Let  $\mathcal{L} \in \mathbf{R}^{L_x L_y \times L_x L_y}$  denote a graph Laplacian on this grid, where coupling strengths between adjacent cells are drawn independently from a uniform distribution on the interval  $[w_0, w_1] \subset \mathbf{R}$ . We first consider the following Markovian linear dynamical system:

$$\mathbf{x}_{t+1} = \mathcal{A}\mathbf{x}_t + \mathcal{B}\mathbf{u}_t, \quad \mathbf{x}_0 = \mathbf{0}_{L_x L_y \times 1}, \quad (34)$$

where  $\mathcal{A} := \mathbb{1}_{L_x L_y} + \mathcal{L}h$  and  $\mathcal{B} := \mathbb{1}_{L_x L_y} h$ , with time step  $h > 0$ . The input sequence  $\{\mathbf{u}_t\}_{t \geq 0}$  represents external actuation.

To model memory effects arising from system–reservoir interactions, we also consider a non-Markovian extension. Specifically, we set  $A = \mathcal{A}$ ,  $B = \mathcal{B}$ , and introduce a memory kernel matrix  $D = \mathcal{D}$  in Definition 6, with given integers  $m > q \geq 0$  and  $\mathcal{D} \in \mathbb{T}_m^q(Q)$ . Such memory effects naturally arise in systems coupled to unobserved degrees of freedom such as external reservoirs [14].

Throughout the experiments, we fix  $L_x = 20$ ,  $L_y = 5$ ,  $n = L_x L_y = 100$ ,  $k = n$ ,  $m = 1,000$ ,  $h = 1/(m-1)$ ,  $w_0 = 0.5$ ,  $w_1 = 1.5$ ,  $q = 2$ ,  $Q = 3$ , and

$$D = \begin{pmatrix} 0 & 0 & -0.01 & 0 & \dots \\ 0 & 0 & 0.03 & -0.01 & \\ 0 & 0 & 1 & 0.03 & \\ \vdots & & & & \end{pmatrix} \in \mathbb{T}_m^q(Q). \quad (35)$$

Define a matrix  $U_{\sigma, \nu, \xi}^* = (u_{it}) \in \mathbf{R}^{n \times m}$  as follows: for  $t = 0, 1, 2, \dots$ , spatial coordinates  $x, y$ , and  $i \in [n]$ ,

$$u_{it} = \begin{cases} \sigma^x \delta_{\xi, y} \sin(2\pi \nu t h) & \bullet = \parallel \\ \sigma^y \delta_{\xi, x} \sin(2\pi \nu t h) & \bullet = \perp \end{cases}. \quad (36)$$

Note that, in the Markovian case with zero control input, the energy is conserved. We define the energy at time  $t$  as

$$E(t) = \frac{1}{n} \sum_{i \in [n]} (\mathbf{x}_t)_i. \quad (37)$$

### B. Train and Test Datasets

We generate train, test and energy test sets by using the following sets of pairs of control inputs and initial values  $(U, (\mathbf{x}_0 \ \mathbf{x}_1 \ \dots \ \mathbf{x}_q))$  as follows:

$$\mathcal{S}_{\text{tr}} = \left\{ \left( U_{\sigma, \nu, \xi}^{\parallel}, 0_{n \times q} \right) \mid \sigma = \pm 1, \nu \in \{3, 6\}, \xi \in [5] \right\}, \quad (38)$$

$$\mathcal{S}_{\text{ts}} = \left\{ \left( U_{1, \nu, 0}^{\perp}, 0_{n \times q} \right) \mid \nu \in [1, 9] \right\}, \quad (39)$$

$$\mathcal{S}_{\text{en}} = \left\{ (0_{n \times m}, \mathbf{1}_{n \times q}) \right\}, \quad (40)$$

respectively. We assume  $q = 0$  for the Markovian case.

We prepare pairs of train and test datasets both for Markovian (34) and non-Markovian (Definition 6) dynamical systems using (38) and (39). Noisy train data is generated using three independent noise realizations. For each training trajectory  $\tau \in \mathcal{S}_{\text{tr}}$ , the root mean square of the snapshot matrix  $X^{(\tau)}$  is defined as  $\rho_{\tau} := \|X^{(\tau)}\|/\sqrt{nm}$ , and additive Gaussian noise with standard deviation  $\sigma = 0.05 \times \max_{\tau \in \mathcal{S}_{\text{tr}}} \rho_{\tau}$  is applied to the state observations, while no noise is added to the test datasets  $\mathcal{S}_{\text{ts}}$  and  $\mathcal{S}_{\text{en}}$ .

### C. Constraints and Learning

We use following constraints A1 or A2 and B to identify the coefficient matrices  $A, B$ :

A1  $A^{\top} = A$ ,  $A_{ij} = 0$  if  $j \notin N_i$ , and off-diagonal elements of  $A$  are nonnegative

A2  $A$  is a graph Laplacian,  $A_{ij} = 0$  if  $j \notin N_i$ , and off-diagonal part of  $A$  is nonnegative

B  $B$  is a diagonal matrix whose elements are nonnegative  
For A2, we used Algorithm 4 in [11] to construct the convex projection onto the set of (asymmetric) graph Laplacians.

In the learning procedure, we set  $t_0 = 0.3$ ,  $\eta = 1.05$ ,  $\theta^{(0)} = (\mathbb{1}_n, 0_{n \times k}, \mathbb{1}_m)$ , and  $p = 10,000$  in Algorithm 1.

### D. Modeling using DMDc and DMDm

We use DMDc [9] and DMDm [1] as baseline methods. For both methods, no rank truncation or dimensionality reduction is applied, since truncation based on train data would bias the identified models toward the excited subspace and impair generalization under partial excitation.

DMDc is applied under the Markovian assumption disregarding the memory effect using a multi-trajectory formulation (Section III-C), while DMDm does not naturally admit multi-trajectory identification and is therefore fit independently to each training trajectory, with a single representative model constructed by element-wise averaging of the estimated coefficients.

### E. Results

This section reports numerical results evaluating NOMADS in terms of prediction accuracy, physical consistency, and optimization behavior under partially excited experimental settings.

### 1) Overview of computational cost and prediction accuracy:

Table II reports modeling time (average over 3 trials for noisy data), prediction RMSE (root mean squared error), and, for the Markovian case, the maximum absolute energy error. Across both Markovian and non-Markovian settings, NOMADS achieves substantially smaller test reconstruction errors than DMD-based baselines.

The symmetry constraint (A1) generally yields lower RMSE, whereas the graph Laplacian constraint (A2) more accurately preserves energy in the Markovian case.

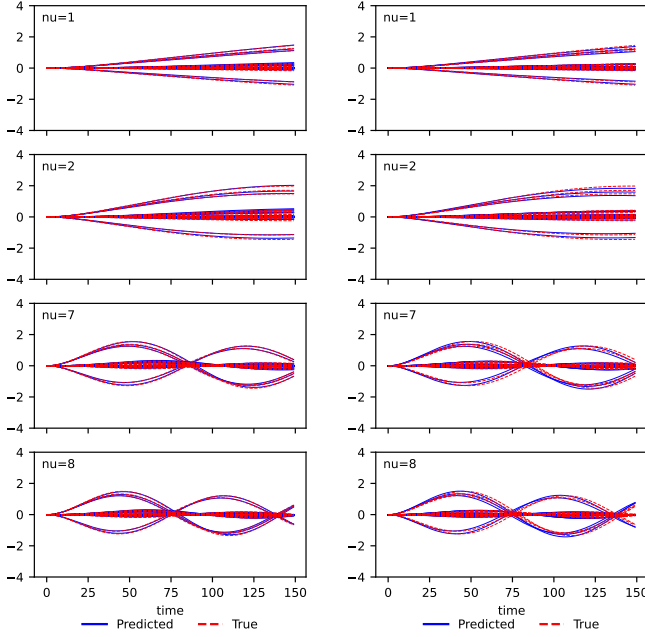


Fig. 1. NOMADS with A2 and B constraints for the non-Markovian dynamical system. Comparison between the ground truth (solid lines) and reconstructed trajectories (dotted lines), evaluated on  $\mathcal{S}_{t_s}$ . Left column: models trained on noiseless training data. Right column: models trained on noisy training data.

**2) Reconstruction results:** Figures 1 and 2 compare reconstructed trajectories with the ground truth for both Markovian and non-Markovian systems. NOMADS accurately reproduces the long-term dynamics in both noiseless and noisy training settings, whereas DMD-based methods exhibit significant deviations, particularly for non-Markovian dynamics, even when trained on noiseless data.

**3) Energy conservation:** Figure 3 shows the time evolution of the energy error in the Markovian setting, where energy conservation holds. The models are trained on noiseless data. NOMADS with the graph Laplacian constraint (A2) achieves the smallest energy error.

**4) Learning curves:** Figure 4 shows the learning curves of NOMADS. In the non-Markovian cases, the loss decreases rapidly in early iterations and then converges gradually, reflecting the effect of projection onto the feasible set of causal memory kernels.

## F. Discussion

This section discusses the numerical results in light of the three challenges identified in the introduction: (i) generaliza-

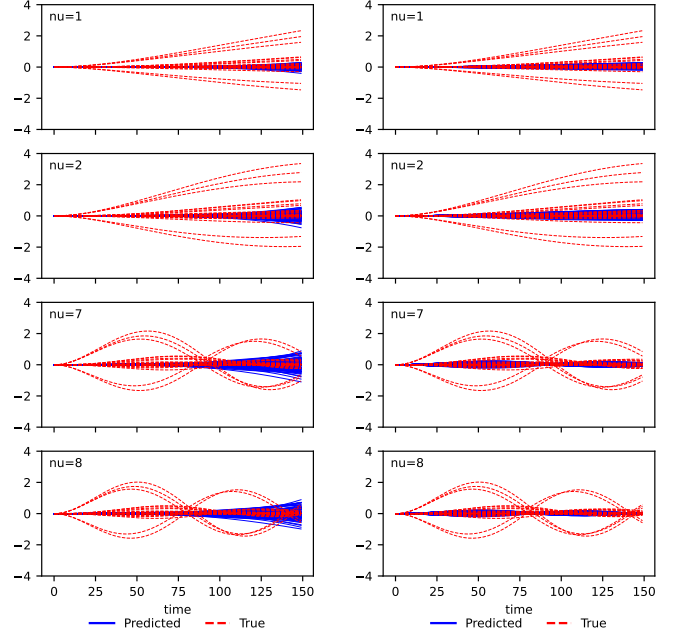


Fig. 2. Existing methods. Ground truth (solid) and reconstructed trajectories (dotted) for the Markovian dynamical system. Models are identified from noiseless train data  $\mathcal{S}_{t_r}$  and evaluated on  $\mathcal{S}_{t_s}$ . Left: DMDm. Right: DMDc trained on horizontally concatenated trajectories.

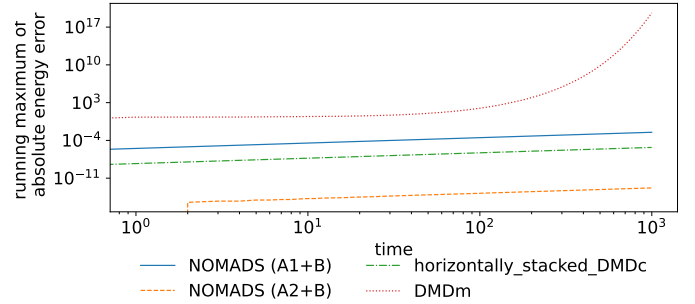


Fig. 3. Running maximum of the absolute energy error in the Markovian settings, where the energy  $E(t)$  is defined in (37). The initial condition is set to  $\mathbf{x}(0) = \mathbf{1}_{n \times 1}$ . All models are trained on noiseless training data.

tion under partial excitation, (ii) physical consistency through constraints, and (iii) modeling of non-Markovian dynamics. As emphasized earlier, the first two challenges are closely related and are addressed through multi-trajectory learning with physical constraints, while the third concerns the expressiveness of the dynamical model itself.

First, regarding reconstruction accuracy under partial excitation, NOMADS consistently achieves smaller test errors than DMD-based methods in both Markovian and non-Markovian settings. Since the test trajectories differ qualitatively from the train data, this improvement indicates genuine generalization rather than overfitting. In contrast, DMDc and DMDm suffer from large errors, reflecting the non-identifiability issues discussed in Section III-C.

Second, in the Markovian case, NOMADS with the graph Laplacian constraint improves energy conservation, while that with symmetry constraints tend to reduce reconstruction error. This highlights a trade-off between numerical accuracy and

TABLE II  
COMPUTATIONAL COST AND PREDICTION ACCURACY.

Method	Modeling Time [s]	Markov			Non-Markov	
		RMSE (noiseless)	RMSE (noisy)	Max absolute energy error	RMSE (noiseless)	RMSE (noisy)
DMDc [9]	<b>0.89</b>	0.33	$(2.20 \pm 2.01) \times 10^{12}$	$5.01 \times 10^{-6}$	$5.85 \times 10^{104}$	$(7.12 \pm 4.62) \times 10^{11}$
DMDm [1]	5.45	$3.11 \times 10^{17}$	$(5.07 \pm 7.14) \times 10^{10}$	$4.33 \times 10^{19}$	NaN	NaN
NOMADS (A1+B)	$2.99 \times 10^4$	<b><math>1.06 \times 10^{-2}</math></b>	<b><math>(1.12 \pm 0.0015) \times 10^{-1}</math></b>	$3.20 \times 10^{-3}$	<b><math>1.02 \times 10^{-2}</math></b>	<b><math>(2.86 \pm 0.025) \times 10^{-2}</math></b>
NOMADS (A2+B)	$2.87 \times 10^4$	$5.28 \times 10^{-2}$	$(1.43 \pm 0.027) \times 10^{-1}$	<b><math>1.57 \times 10^{-13}</math></b>	$2.92 \times 10^{-2}$	$(3.51 \pm 0.046) \times 10^{-2}$

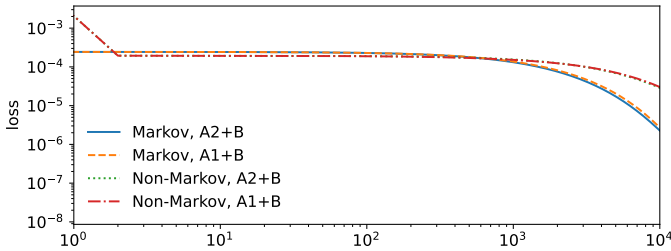


Fig. 4. Learning curves of the training loss for NOMADS under different constraints. All models are trained on noiseless training data.

strict enforcement of physical structure, depending on the constraint design.

Third, NOMADS remains effective in the non-Markovian setting with noisy train data, where standard DMD-based approaches fail to capture memory effects. By explicitly incorporating a memory kernel into the optimization framework, NOMADS yields stable long-term predictions even when individual trajectories are only partially excited.

Finally, in the present setting, the underlying physical dynamics suggests that a symmetric graph Laplacian constraint would be the most natural choice. Efficient projection onto the set of symmetric graph Laplacians remains computationally challenging. While projection-based methods such as those of Sato *et al.* [11] are principled, their repeated use within an iterative optimization framework like NOMADS would incur substantial computational overhead, and is therefore left for future work.

## VI. CONCLUDING REMARKS

In this paper, we proposed NOMADS (Non-Markovian Optimization-based Modeling for Approximate Dynamical Systems with Spatially-homogeneous memory), a system identification framework for dynamical systems using collections of partially excited experiments. NOMADS integrates multiple trajectories, incorporates homogeneous memory effects, and enforces physically motivated constraints within a convex optimization formulation.

We established convergence guarantees for the projected gradient-based algorithm used in NOMADS and demonstrated its effectiveness through numerical experiments using synthetic data. The results show that NOMADS achieves lower reconstruction errors on test data than DMD-based methods even for non-Markovian systems with noisy train data, indicating improved generalization performance measured in terms

of test-set reconstruction accuracy. In our experiments, the training and test experiments are intentionally qualitatively different, highlighting the robustness of the proposed framework.

Moreover, incorporating physically motivated constraints contributes both to improved reconstruction accuracy and to the preservation of physical properties such as conservation laws.

These results indicate that NOMADS provides a reliable and flexible approach for identifying high-dimensional non-Markovian dynamical systems under partial excitation.

## ACKNOWLEDGMENT

The authors thank Mr. Ren Sasaki (Equipment Intelligence & App R&D Department, Tokyo Electron Ltd.) for his assistance with the numerical computations of DMDm. This work was partly supported by Japan Society for the Promotion of Science KAKENHI under Grant 23K28369.

## APPENDIX I

### LINEAR DYNAMICAL SYSTEMS WITH HOMOGENEOUS MEMORY AND FRACTIONAL DYNAMICS

The time-evolution model in fractional DMD [1] is a fractional-order ordinary differential equation with a positive order  $\alpha > 0$ :

$$\frac{d^\alpha \mathbf{x}}{dt^\alpha} = A\mathbf{x}(t) + B\mathbf{u}(t). \quad (41)$$

Note that the fractional derivative  $\frac{d^\alpha}{dt^\alpha}$  is represented as the composition of integer-order and fractional derivatives as  $\frac{d^\alpha}{dt^\alpha} = \frac{d^{n_\alpha}}{dt^{n_\alpha}} \frac{d^{\alpha-n_\alpha}}{dt^{\alpha-n_\alpha}}$  with  $n_\alpha$  being the minimum positive integer such that  $n_\alpha - \alpha > 0$ . The kernel of the original operator  $\frac{d^\alpha}{dt^\alpha}$  is equivalent to the kernel of the integer-order derivative  $\frac{d^{n_\alpha}}{dt^{n_\alpha}}$ , i.e.,

$$\ker \left( \frac{d^\alpha}{dt^\alpha} \right) = \text{span} \{ t^\ell | \ell \in [n_\alpha] \}. \quad (42)$$

Therefore, we multiply the pseudoinverse operator  $\frac{d^{-\alpha}}{dt^{-\alpha}}$  from left to the both sides of the above equation to yield

$$\mathbf{x}(t) - \sum_{\ell=0}^{n_\alpha} \mathbf{x}_0^{(\ell)} t^\ell = \frac{d^{-\alpha}(A\mathbf{x} + B\mathbf{u})}{dt^{-\alpha}}, \quad (43)$$

where  $\mathbf{x}_0^{(\ell)} \in \mathbf{R}^n$  is the  $\ell$ th derivative of  $\mathbf{x}(t)$  at  $t = 0$ .

In the discrete time representation for given time points  $(t_i)_{i \in [m]}$  with equal spacing  $\Delta t := t_{i+1} - t_i$ , the fractional-order derivative is represented by a  $m$ -dimensional time-invariant causal matrix  $D_\alpha \in \mathbf{R}^{m \times m}$  which satisfies the following conditions:

- 1)  $D_0 = \mathbb{1}_m$ ,
- 2)  $(0^b \ 1^b \ \dots \ (m-1)^b)D_a = 0_{n \times m}$  for integers  $b < a$ ,
- 3)  $D_\alpha D_\beta = D_{\alpha+\beta}$  for  $\alpha, \beta > 0$ .

We can show that  $\ker(D_\alpha^\top) = \ker(D_{n_\alpha}^\top) = \text{span} \{ [v_i] \in \mathbf{R}^m \mid v_i = (t_i)^\ell, i \in [m], \ell \in [n_\alpha] \}$ . Noting that the discretization induces  $\frac{d^\alpha}{dt^\alpha} \rightarrow D_\alpha^+$ , we can see that this is a special case of general memory kernel matrix.

## APPENDIX II

### UNIQUENESS IN DMD, DMDc, AND NOMADS

In this section, we focus on the uniqueness of the NOMADS, MTDM, and DMDc. There are limited attentions [7] on the uniqueness, but in our *from-analysis-to-identification* perspective, the uniqueness of the coefficient is of utmost interest.

*Theorem 18 (Uniqueness in NOMADS):* Under the settings of Theorem 14, assume that  $\text{St}(A) = \mathbf{R}^{n \times n}$ ,  $\text{St}(B) = \mathbf{R}^{n \times k}$ ,  $\text{St}(D) = \mathbb{T}_m^q$ . The optimization problem (16) has a unique minimizer if and only if the Hessian (21) is a positive definite operator.

If  $D$  is fixed, the theorem becomes simpler:

*Theorem 19 (Uniqueness in Multi-trajectory DMDm):*

Under the settings of Theorem 14, further assume that  $\text{St}(A) = \mathbf{R}^{n \times n}$ ,  $\text{St}(B) = \mathbf{R}^{n \times k}$ ,  $\text{St}(D) = \{D\}$  for a given matrix  $D \in \mathbf{R}^{m \times m}$ . The optimization problem (16) has a unique minimizer if and only if the Hessian (25) is a positive definite matrix.

*Corollary 20 (Uniqueness in DMDc):* Under the settings of Theorem 19, let us further assume  $N = 1$  and  $D = \mathbb{1}_m$ . This setting is corresponding to DMDc. The optimization problem (16) has a unique minimizer if and only if

$$\text{rank} \begin{pmatrix} X \\ U \end{pmatrix} = n + k. \quad (44)$$

Note that, the above equality is satisfied only if  $m \geq n + k$ .

*Proof:* In this case the Hessian becomes a  $(n + k)$ -dimensional square matrix (25):

$$\text{Hess}f(A, B) = \begin{pmatrix} XX^\top & XU^\top \\ UX^\top & UU^\top \end{pmatrix} = \begin{pmatrix} X \\ U \end{pmatrix} \begin{pmatrix} X \\ U \end{pmatrix}^\top. \quad (45)$$

Noting that  $\text{Hess}f(A, B)$  is a positive semidefinite symmetric matrix, and is positive definite if and only if it further satisfies  $\text{rank}(\text{Hess}f(A, B)) = n + k$ . Using the fact that  $\text{rank}(C) = \text{rank}(CC^\top)$  for any real-valued matrix, one can conclude that  $\text{rank} \begin{pmatrix} X \\ U \end{pmatrix} = n + k$  is the necessary and sufficient condition for the uniqueness. ■

*Remark 21:* The minimizer of the optimization problem (16) with fixed  $D$  is not unique in a single-trajectory case if  $m < n + k$ , and the minimizer is unique if and only if the data matrix (i.e.,  $X$  for DMD,  $(X \ U)$  for DMDc) has no left null-space. This means that, in many applications, the DMD and DMDc algorithm easily results in unphysical coefficients, especially if the number of time steps are small.

On the other hand, for the same optimization problem with  $N > 1$ , the Hessian can be positive definite even if the minimum number of time steps  $\min_\mu(m_\mu)$  is smaller than the combined dimension  $n + k$  provided we have appropriate set of trajectories.

## REFERENCES

- [1] R. Anzaki *et al.* “Dynamic mode decomposition with memory”. In: *Physical Review E* 108.3 (2023), p. 034216.
- [2] R. Anzaki *et al.* “Multi-trajectory Dynamic Mode Decomposition”. In: *Jxiv preprint* (2024).
- [3] K. J. Åström and P. Eykhoff. “System identification—a survey”. In: *Automatica* 7.2 (1971), pp. 123–162.
- [4] A. Beck. *First-order methods in optimization*. SIAM, 2017.
- [5] D. Bertsekas. *Nonlinear Programming: 3rd Edition*. Athena Scientific, 2016.
- [6] G. C. Goodwin, S. F. Graebe, M. E. Salgado, *et al.* *Control system design*. Vol. 240. Prentice Hall Upper Saddle River, 2001.
- [7] S. M. Hirsh *et al.* “Centering Data Improves the Dynamic Mode Decomposition”. In: *SIAM Journal on Applied Dynamical Systems* 19.3 (2020), pp. 1920–1955.
- [8] Yurii Nesterov. *Introductory Lectures on Convex Optimization: A Basic Course*. Kluwer Academic Publishers, 2004. ISBN: 978-1-4020-7786-9.
- [9] J. L. Proctor, S. L. Brunton, and J. N. Kutz. “Dynamic mode decomposition with control”. In: *SIAM Journal on Applied Dynamical Systems* 15.1 (2016), pp. 142–161.
- [10] A. W. Roberts and D. E. Varberg. *Convex Functions: Convex Functions*. Academic Press, 1974.
- [11] K. Sato and M. Suzuki. “The nearest graph Laplacian in Frobenius norm”. In: *Numerical Linear Algebra with Applications* (2024), e2578.
- [12] P. J. Schmid. “Dynamic Mode Decomposition and Its Variants”. In: *Annual Review of Fluid Mechanics* 54.1 (2022), pp. 225–254.
- [13] P. J. Schmid. “Dynamic mode decomposition of numerical and experimental data”. In: *Journal of fluid mechanics* 656 (2010), pp. 5–28.
- [14] Adam Svenkeson *et al.* “Spectral decomposition of nonlinear systems with memory”. In: *Phys. Rev. E* 93 (2 2016), p. 022211.
- [15] J. H. Tu *et al.* “On dynamic mode decomposition: Theory and applications”. In: *Journal of Computational Dynamics* 1.2 (2014), pp. 391–421.